Breaking the Color Barrier: A Multi-Selective Antibody Reporter Offers Innovative Strategies of Fluorescence Detection

Eugenio Gallo [†], and Jonathan W. Jarvik [†,§]

[†] Department of Biological Sciences,
Carnegie Mellon University, Pittsburgh, Pennsylvania, USA 15213
[§] Molecular Biosensor and Imaging Center,
Carnegie Mellon University, Pittsburgh, Pennsylvania, USA 15213

Corresponding Author: Eugenio Gallo, PhD
Carnegie Mellon University
4400 Fifth Ave.,
MI 257
Pittsburgh, Pennsylvania, 15213
Phone: (412) 268-3398
Fax: (412) 268-6571
E-mail: gino.gallo@utoronto.ca

Summary Statement: We present a multi-color bipartite protein reporter for cell-surface labeling of receptors. Here we highlight innovative strategies of detection previously difficult or impossible with conventional fluorescent systems.

Journal of Cell Science • Advance article

JCS Advance Online Article. Posted on 14 June 2017

Abstract

A novel bi-partite fluorescence platform exploits the high affinity and selectivity of antibody scaffolds to capture and activate small molecule fluorogens. In this report we investigated the property of multi-selectivity activation from a single antibody against diverse cyanine-family fluorogens. Our fluorescence screen identified three cell impermeant fluorogens; each with unique emission spectra (blue, green, and red) and nanomolar affinities. Most importantly, as a protein fusion-tag to G-protein-coupled receptors the antibody biosensor retained full activity – displaying bright fluorogen signals with minimal background on live cells. Because fluorogen-activating antibodies interact with their target ligands via non-covalent interactions we were able to perform advanced multi-color detection strategies on live cells, previously difficult or impossible with conventional reporters. That is, by fine-tuning the concentrations of the different color fluorogen molecules in solution a user may alternate fluorescence (signal onset versus offset), execute real-time signal exchange via fluorogen competition, measure multi-channel fluorescence via co-labelling, and perform real-time cell surface receptor traffic via pulse-chase. Thus, here we inform of an innovative reporter technology based on tri-color signal that allows user-defined fluorescence tuning in live cell applications.

Keywords: Antibody/Biosensor/FAP/Fluorescence/Fluorogen /scFv

Introduction

Fluorescence protein reporters have dramatically transformed the probing methods for discerning cellular and molecular phenomena. In more detail, this fluorescence revolution commenced with the gene sequence identification and molecular cloning of the jellyfish *Aequorea victoria* fluorescent protein (Prasher et al., 1992; Shimomura et al., 1962), and was followed with other animal models (Masuda et al., 2006; Matz et al., 1999; Shagin et al., 2004). Such isolated fluorescent proteins were often bioengineered as functional reporter tags in living cells – with features of improved thermal stabilities, multi-detection wavelengths, bipartite split-domains, and environmental sensing probes to highlight a few (Cabantous et al., 2005a; Cabantous et al., 2005b; Kent et al., 2009; Sample and Newman, 2009; Shaner et al., 2004; Shaner et al., 2005). Until today fluorescence biosensors form an indispensable arsenal for every sector of biological research – academia, industry, and medicine. Accordingly, their application, developability, and influence will further continue in this new century, with innovative technologies already emerging.

In the past decade, novel biosensing reporter approaches started to challenge the conventional paradigm of fluorescent proteins. That is, scientists started to explore bio-conjugate platforms where fluorescent modalities and protein scaffolds would interact to form stable complexes. Here, some researchers identified and developed protein scaffolds that form covalent interactions with small molecule fluorescent ligands via chemical or enzymatic coupling mechanisms. As a result, such bipartite reporters offered enhanced spatial and temporal resolutions at the surface of cells and/or intracellular milieu (Chen et al., 2005; Fernández-Suárez et al., 2007; Gautier et al., 2008; Griffin et al., 1998; Hori et al., 2009; Keppler et al., 2002; Keppler et al., 2004; Los et al., 2008; Luedtke et al., 2007). More advanced approaches utilized the capture of fluorogenic molecules, which are inherently non-fluorescent unless sterically restricted. The most successful of these to date is called fluorogen-activating proteins (FAPs), and utilizes the high affinity and selectivity of antibodies to form stable non-covalent bonds with target fluorogens (Szent-Gyorgyi et al., 2008). Here the

antibody functions as a protein cage that sterically confines the small molecule, and upon light excitation the fluorogen emits fluorescence – due to the release of non-radiative energy decay. Incidentally, FAP technology also offers a malleable approach for altering fluorescence signals; primarily by modifying the chemical composition of the synthetic fluorogens in order to tune their binding affinities and/or spectra (Pham et al., 2015; Rastede et al., 2015; Saunders et al., 2013; Saunders et al., 2014; Szent-Gyorgyi et al., 2010). Furthermore, FAP reporters have demonstrated a rapid advancement as tools for labelling cellular targets at the surface (Fig. S1), showing absence of intracellular background/noise and high cell surface signal brightness comparable to (or greater) than conventional fluorescent proteins (Holleran et al., 2010; Saunders et al., 2012; Szent-Gyorgyi et al., 2008; Szent-Gyorgyi et al., 2010).

The majority of current fluorescence protein technologies show lack of multi-color detection and signal modulation. Some breakthroughs occurred in the covalent bio-conjugate field where the same target ligand for capture may be chemically coupled with unique color fluorophores, a very similar approach to using commercially labelled antibodies for labelling cells (Irwin Chen et al., 2007; Kosaka et al., 2009; Laura Vivero-Pol et al., 2005; Lee et al., 2010; Liu et al., 2014; Uttamapinant et al., 2010; Wombacher et al., 2010; Yao et al., 2012). Likewise, other groups have utilized bio-conjugate platforms based on tandem dye interactions that have resulted in FRET, a donor-acceptor approach that amplifies the Stokes shift of a molecule resulting in fluorescence emissions at longer wavelengths (Brun et al., 2009; Brun et al., 2011; Gallo et al., 2015; Pham et al., 2015; Rajapakse et al., 2010; Robers et al., 2009; Saunders et al., 2014; Yushchenko et al., 2012; Zürn et al., 2010). As a result, we find that current methods prove lacking in multi-color detection and real-time signal modulation. In this regard, FAP technology may prove better capable for generating multi-fluorescence detection from a single reporter, due to the non-covalent nature of the affinity interactions.

Recently, a group isolated a multi-selective single-chain-variable-fragment (scFv) with affinity activation for various cyanine family fluorogens with differing poly-methine group lengths (Özhalici-Ünal et al., 2008). In summary, this work showed that a scFv FAP may display binding

promiscuity with different small molecule fluorogens analogs. Inspired by this observation, we set out to screen a previously isolated scFv FAP for multi-fluorogen activation against a family of small molecule variants. Thus, we explored fluorogens with assorted structural and electrostatic properties, with aim to isolate fluorogens with diverse spectra. As a result, our affinity screen identified three cell impermeant fluorogens with sub-micromolar affinities for the scFv scaffold. Most importantly each fluorogen possesses a unique spectra that results in coverage of the entire visible spectrum from a single fluorescent reporter. As a result, we further explored advanced multi-color fluorescence detection at the surface of live cells. We investigated fluorescence signal manipulation via fluorogen removal and addition, multi-color target detection via co-labeling, and real-time fluorescence color-switch via affinity binding competition. To further highlight the potential of a multi-color scFv reporter, we tracked in real-time the cell surface internalization of a G-protein-coupled receptor via tri-color pulse-chase using live cells.

Thus, when compared to conventional systems, where signal is ever-present and monochromatic (such as fluorophore labelled antibodies or fluorescent proteins), our findings show that a multi-selective affinity biosensor expands the opportunities of detection, resulting in user-defined spatial and temporal resolutions. In brief, here we report of a multi-color scFv FAP and demonstrate its importance for fluorescence detection on live-cells.

Experimental Procedures

Plasmid Constructions. The surface expression of scFvs HL1.0.1-TO1 and HL1-TO1 (Fig. S2) fused N-terminal to adrenoreceptor-beta-2 (ADRB2) on mammalian cells was performed using the pDisplaySacLac2 plasmid (Holleran et al., 2010). HL1.0.1-TO1 and HL1-TO1 gene inserts (Szent-Gyorgyi et al., 2008) were PCR amplified to include a 5' *SfiI* restriction site sequence GGCCCAGCCGGCC and 3' *SfiI* restriction site sequence GGCCGCAGGGGCC, and each insert cloned into a *SfiI* enzyme digested pDisplaySacLac2. Subsequently, a complete ORF and stop codon from the ADRB2 gene, encoding the b2AR receptor, was PCR amplified (template: fosmid WI2-2202O9/G248P86156H5, BACPAC Resources Center, Oakland CA) to include 5' and 3' *BsmI*

restriction sites using primer sequences GATCTGAATGCTATGGGGCAACCCGG and CCCACAGCATTCTACAGCAGTGAGTCATTTCTACTACAATT, as previously shown (Fisher et al., 2010), and cloned into *BsmI* enzyme digested pDisplaySacLac2.

Cell Lines and Culture Conditions. We utilized a JAR200 yeast cell line (Mat a ura3-52, trp1, leu2δ200, his3δ200, pep4:HIS3, prbd1.6R, can1, GAL, GAL promoter-AGA1::URA3:G418r) for the surface display of HL1-TO1 or HL1.0.1-TO1 scFvs using methods previously described (Szent-Gyorgyi et al., 2008). Also, we utilized a HEK-293 mammalian cell line (ATCC, Manassas, Virginia, USA) for all transient plasmid transfections using reagent TransIT®-LT1 (Mirus Bio, Madison, Wisconsin, USA) according to the manufacturer's instructions. The mammalian cells were grown at 37°C, 5% CO2 in Dulbecco's modified Eagle's medium (DMEM) plus 10% fetal calf serum, 100 U/mL penicillin and 100 µg/mL streptomycin.

Protein Expression and Purification. Purified HL1.0.1-TO1 scFv protein was obtained using a Rosetta-Gami *E.coli* strain (Novagen, Billerica, Massachusetts, USA), where the cells were induced with 0.5 mm isopropyl-β-d-thiogalactopyranoside (RPIcorp, Prospect, Illinois, USA), lysed, and pelleted via high-speed centrifugation. The supernatant was used in nickel-nitrilotriacetic acid chromatography (Ni-NTA; Thermo-Fisher, Waltham, Massachusetts, USA) according to the manufacturer's instructions. The eluted fractions were purified via gel-filtration chromatography, then pooled, and concentrated using centrifugal-filter units (EDM Millipore, Billerica, Massachusetts, USA). The final scFv protein concentration was determined by spectroscopy measured at 280 nm wavelength and calculated using the Beer-Lambert equation. The protein samples were aliquoted and stored in phosphate-buffered-saline (PBS) with 0.09% sodium azide at -20 Celsius. All thawed samples were subsequently stored at 4 Celsius for one month, and then discarded.

Optical Spectroscopy Assays. The samples were analyzed in an Infinite M1000 plate spectrometer (TECAN, Männedorf, Switzerland) using transparent, flat-bottom, 96-well microtiter plates (Corning, Corning, New York, USA). For the fluorogen activation screen the fluorescence measurements were performed in triplicate using 0.5 µM purified scFv protein and fluorogen in 200

µL of PBS. The emission spectra comparisons between HL1-TO1 and HL1.0.1-TO1 were determined using triplicate samples of 10^6 surface-displayed scFv yeast cells in 200 µL of PBS, and corrected for background fluorescence using wild-type control cells. For correct comparisons the fluorogens were presented at same Kd concentration values, where 2-fold Kd for OTB-SO3 and DIR and 5-fold Kd for TO1-2p (see Table 1). All kinetic titration measurements were determined using yeast surface displayed HL1.0.1-TO1 in triplicate samples and fluorogen titrated at different concentrations and corrected for background fluorescence using wild-type control cells. The data were fit to a one-site binding equation (Fig. S5) using Graph-pad Prizm 5.0 (GraphPad Software, San Diego, California, USA), where x is the fluorogen concentration:

$$y = Bmax * x\ /(Kd + x)$$

Fluorescence Microscopy. The images were acquired with a Carl Zeiss LSM 510 Meta/ UV DuoScan inverted confocal microscope using a 405 nm laser and a 430-480 nm band-pass filter for OTB-SO_3 fluorogen, a 488 nm laser and a 505-550 nm band-pass filter for TO1-2p fluorogen, and a 561nm laser and 575 nm LP band-pass filter for DIR fluorogen. Cells were imaged in PBS using 35-mm glass-bottom dishes (MatTek, Ashland, Massachusetts, USA), and images analyzed using ImageJ software (http://rsb.info.nih.gov/ij/).

Cell Surface Imaging Assays. HEK293 cells transiently expressing HL1.0.1-TO1 fused to ADRB2 were labelled with 100 nM OTB-SO_3, TO1-2p, or DIR fluorogens. For evaluating signal loss by fluorogen removal, the cells were presented with fluorogen in the medium and incubated for 10 minutes at room temperature. Subsequently the cells were washed with PBS plus Ca/Mg and immediately imaged using time-lapse microscopy at 15 second intervals for 10 minutes. Next, the cells were presented again with fluorogen and imaged. For evaluating signal exchange via fluorogen competition, the cells were presented with OTB-SO_3 fluorogen in the medium and incubated for 10 minutes. Subsequently, either TO1-2p or DIR fluorogens were added and the cells were immediately imaged using time-lapse microscopy at 15 second intervals for 10 minutes. For evaluating receptor traffic via agonist stimulation, initially 100 nM of DIR fluorogen was added to the cellular medium and the cells imaged after 5 minutes incubation with the fluorogen. Following, a final concentration

of 10 μM isoproterenol (Sigma-Aldrich, St. Louis, Missouri, USA) was added to the medium and the cells were incubated for 30 min. at 37°C. Following, the cells were re-imaged. The media was then removed, the cells gently washed with PBS plus Ca/Mg and media re-added with 100 nM OTB-SO_3 fluorogen. Following, the cells were re-imaged after incubation for 5 minutes with the fluorogen. Next, a final concentration of 10 μM isoproterenol was added to the medium and the cells were incubated for 30 min. at 37°C, and subsequently the cells were re-imaged. Following, the media was removed; the cells were gently washed with PBS plus Ca/Mg, and cell media was re-added with 100 nM TO1-2p fluorogen. Subsequently, after 5 minutes the cells were re-imaged.

Cellular Fluorescence Photobleach Assay. HEK293 cells transiently expressing HL1.0.1-TO1 fused to ADRB2 were imaged in presence of either 100 nM OTB-SO_3, TO1-2p, or DIR fluorogens. The cells were photobleached over four Z-stack planes for a total of 20 cycles that consisted 30 second iterations of 10% laser power (a 405 nm laser for OTB-SO_3, a 488nm laser for TO1-2p, or a 561 nm laser for DIR). Fluorescence microscopy acquisition was performed between each cycle, while maintaining the same settings across each fluorogen group. Image fluorescence values from each Z-stack were converted to maximum intensity averages onto a single image. Subsequently, the fluorescence values for each image cycle were normalized to the initial image (pre-photobleaching) for analysis comparisons.

Results

Assessment of Multi-Fluorogen Activation from scFv HL1.0.1-TO1

We set up a fluorescence activation fluorogen screen using diverse cyanine family fluorogens against a previously isolated scFv, called HL1.0.1-TO1, with known specificity for a Thiazole-Orange fluorogen derivative (Szent-Gyorgyi et al., 2008). In our screen we included small molecule analogs with variances in structural and physico-chemical properties. More specifically, we screened fluorogens with altered polymethine-group lengths, atomic substitutions, electrostatic alterations, altered molecular polarities, and removal/addition of subgroups at distinct spatial locations. Incidentally, the molecular screening method utilized purified scFv protein in the presence of fluorogen, and was biased for high-affinity interactions with measurements at sub-micromolar concentrations of each moiety.

Figure 1A compares normalized activation of Thiazole-Orange (TO) and analog derivatives TO1, TO2, and TO1-2p. We observed improved fluorescence emission when a negative charged subgroup was present at the benzothiazole ring position, such as in TO versus TO1 or TO1-2p, while the same addition to the quinoline ring of TO substantially reduced fluorescence emission, such as TO versus TO2. On the other hand, the addition of diethylene-glycol-diamine (neutral charge group) at the quinoline ring position did not affect fluorescence, such as TO1 versus TO1-2p. Taken together, we observed that molecular electrostatics play a determining role for fluorogen-scFv interactions and their subsequent fluorescence activation.

Fluorine atoms possess strong electron-withdrawing properties. As a result, Fluorine atoms disrupt the electrical polarity of a fluorogen when present in the molecule. In our fluorescence screen we observed diminished activation using different TO fluorogens modified with Fluorine atoms at the benzothiazole ring (Fig. 1B). On the other hand, when measuring the same Fluorine modified fluorogens using an activating medium, such as 90% glycerol, the fluorescence output of the fluorogens remained comparable (Shank et al., 2009). This informs that the fluorogenic

modifications themselves are not intrinsically disruptive. It also highlights that the charge polarity of fluorogens (whole-molecule electrostatics) prove important for directing the affinity interactions with the scFv FAP.

Previous groups demonstrated that a twisted fluorogen conformation may be corrected into a planar geometry inside the binding pocket of a scFv, resulting in fluorescence emission upon excitation (Shank et al., 2013; Silva et al., 2007). As a result, we screened HL1.0.1-TO1 against twisted cyanine fluorogens αCN-TO and αCN-DIR. The data revealed that both fluorogens lack fluorescence activation (Fig. C&D). Incidentally, our results showed a lower signal emission profile for αCN-DIR fluorogen in the presence of protein rather than when free in solution (observed multiple independent times – data not shown). Here we hypothesize that αCN-DIR fluorogen loosely interacts with the scFv protein; yet, its twisted geometry prevents the fluorogen from activating – since a planar conformation is required. Incidentally, the lower observed signal may be attributed to the protein binding pocket encapsulating and shielding the fluorogen from background activation when free in solution. A similar observation was previously identified when measuring the photo-insulating properties of scFv scaffolds and cognate fluorogens (Saurabh et al., 2015; Szent-Gyorgyi et al., 2013). Thus, here we find that HL1.0.1-TO1 lacks the ability to stabilize a twisted conformation into a planar geometry for fluorescence activation.

In Figures 1E-1G we observed that extension of the methine-linker group resulted in decreased or loss of fluorescence signal – such as PO-PRO1 versus PO-PRO3, TO-PRO1 versus TO-PRO5, and YO-PRO1 versus YO-PRO3. Thus, we speculate that the scFv affinity binding region proves restrictive in regards to spatial proximity between the heterocycles. This observation contrast with a previously identified multi-selective scFv (Özhalici-Ünal et al., 2008) – with affinity activation for different fluorogens primarily based on poly-methine group length diversities. As a result, we find some properties are not universal across scFv FAPs and that different antibody scaffolds possess unique affinity requirements in regards to methine-group length extensions.

Additionally we also screened tandem fluorogen molecules, such as TO-TO1 or YO-YO1 fluorogens, for affinity activation against HL1.0.1-TO1. For both molecules we observed robust

emission profiles in presence of the scFv (Fig. 1I). Thus, tandem molecules show fluorogenic activation, regardless of their increased molecular size footprint. As a result, since the scFv HL1.0.1-TO1 was previously isolated against a monomeric fluorogen, we suggest that only one tandem-half of the molecule may actually form the affinity complex – rather than the whole molecule, tandem fluorogen. A similar observation was previously determined when using tandem pairings of fluorogen-fluorophore or fluorogen-polyethylene-biotin molecules (Pham et al., 2015; Szent-Gyorgyi et al., 2010; Vasilev et al., 2016). Here the fluorogen component shows affinity interaction with the scFv irrespective of its tandem fluorogen pair, where most likely both moieties display independent functional activities.

Determining Multi-Fluorogen Activation from scFv HL1.0.1-TO1 and HL1-TO1 at the Surface of Cells

Based on our fluorescence validation screen, we selected three different spectra cell-impermeant fluorogens for further validation on live cells (Fig. S4): Oxazole-Thiazole-Blue derivative (OTB-SO_3) (Zanotti et al., 2011), Thiazole-Orange derivative (TO1-2p), and Dimethyl-Indole-Red (DIR) (Constantin et al., 2008). Also, we included in our assessment scFv HL1.0.1-TO1 versus its parent scFv, HL1-TO1 (non-affinity matured version) (Szent-Gyorgyi et al., 2008). The reasoning behind this was to compare how affinity maturation may influence scFv-fluorogen multi-selectivity and activation, more specifically in regards to fluorescence output and affinity values. As a result, figure 2A shows the fluorescence spectra of each fluorogen in the presence of surface displayed scFvs on yeast cells with measurements acquired at same Kd values for correct comparisons (see Table 1). Accordingly, we observed that all three fluorogens activated in the presence of scFv HL1.0.1-TO1 (as previously identified from our protein screen), while its parent, scFv HL1-TO1, failed to activate OTB-SO_3. Additionally, we also observed improved fluorescence signal from TO1-2p with HL1.0.1-TO1 versus HL1-TO1. On the other hand, HL1.0.1-TO1 showed a lower signal emission profile with DIR rather than HL1-TO1 (parent scFv) – likely due to HL1.0.1-TO1 stricter methine-group length restrictions, as previously identified in Figure 1E-G. Taken

together, affinity matured scFv HL1.0.1-TO1 showed greater binding affinity for all fluorogens when compared to its parent, scFv HL1-TO1 (Table 1). Incidentally, affinity maturation may further explain why HL1.0.1-TO1 activated OTB-SO_3 fluorogen while parent scFv HL1-TO1 failed.

Likewise, the yeast-cell results also corresponded with additional mammalian cell validations utilizing scFv genetic fusions with adrenoreceptor-beta-2 (ADRB2) at the cell surface. Here, we observed abundant and distinct cell surface signal from HL1.0.1-TO1 with all three different color fluorogens independently (Fig. 2B), while the untransfected cells remained dark, indicative of low background/noise from the fluorogens in the medium. On the other hand, parent scFv HL1-TO1 lacked signal activation for OTB-SO_3 fluorogen, and corresponded with our previous yeast-cell assessments. Taken together, scFv HL1.0.1-TO1 demonstrates functional activity as a genetic reporter, showing opportunities of tri-color detection at the surface of live cells.

Evaluating Fluorescence Signal Loss by Fluorogen Removal from the Medium

A property of scFv biosensors is their ability to form non-covalent complexes with their ligands. Hence, fluorogen removal from the cellular medium results in fluorescence signal loss due to the thermodynamically favorable exchange from bound to unbound fluorogen. After first labelling cells tagged with HL1.0.1-TO1 at the cell surface and followed by fluorogen removal, we observed signal loss for all fluorogens (Fig. 3A). Conversely, re-addition of each fluorogen resulted rapid regain of initial fluorescence. Furthermore, some fluorogens exhibited more pronounced signal off-rates than others. That is, TO1-2p fluorogen proved least susceptible to fluorescence signal loss, attributed to HL1.0.1-TO1 high affinity for this fluorogen (see Table 1). Conversely, OTB-SO_3 showed the greatest loss of fluorescence activity when compared to all three fluorogens (Fig. 3B). Note, this proved unexpected since DIR possesses the weakest affinity values for HL1.0.1-TO1 from all three fluorogens (Table 1). As a result, we asked whether photobleaching effects contributed to reduced fluorescence signal over time since fluorogens and fluorophores are susceptible over time exposure to irreversible photochemical alterations that may permanently reduce their ability to fluoresce. We subjected the same cells labelled with each fluorogen to multiple cycles of

photobleaching using identical laser power settings as before. Data analysis showed OTB-SO_3 as the most susceptible fluorogen to photobleaching, while TO1-2p and DIR showed minor sensitivities (Fig. 3C). Accordingly, we repeated the fluorogen removal assay and measured fluorescence at only two time points instead of multiple (such as 15 second intervals for 10 consecutive minutes, see Materials and Methods for descriptive methods) in order to minimize the photobleaching time exposure. The data showed smaller OTB-SO_3 signal loss than prior (over the same time interval) (Fig. 3D). Interestingly, OTB-SO_3 showed comparable values of fluorescence loss as DIR fluorogen, which may indicate of similar ligand off-rates (k-off) for these fluorogens. In conclusion, scFv HL1.0.1-TO1 permits signal manipulation via fluorogen removal from cellular medium; however, photobleaching effects must be taken into consideration for correct assessments.

Assessing Fluorescence Signal Exchange via Fluorogen Competition

In multi-selective settings different fluorogens compete for binding with the same scFv, where the labelling with different fluorogens may result in real-time color exchange. For this analysis we excluded fluorogen competitions between TO1-2p and DIR due to potential Föster-resonance energy transfer (FRET) between these chromophores. We initially labelled the HL1.0.1-TO1 tagged cells with OTB-SO_3 fluorogen and followed by adding TO1-2p or DIR fluorogens to the cellular medium. Time-lapse image analysis showed that majority of OTB-SO_3 signal diminished after TO1-2p fluorogen addition (Fig. 4A). On the other hand, co-labelling was observed when DIR fluorogen was added to the medium (Fig. 4A). For both examples, the data correlates with HL1.0.1-TO1 fluorogen affinity values, where the high scFv affinity of TO1-2p competes for binding and displaces OTB-SO_3 over time (Fig. 4B), while a weaker affinity DIR only partially displaces OTB-SO_3, and after 10 minutes majority of OTB-SO_3 signal remains (Fig. 4C). As previous, in order to assess any contribution of photobleaching effects, we repeated the fluorogen competition assay and measured for fluorescence activation at only two time points instead of multiple. The results showed comparable signal loss for OTB-SO_3 when competed with TO1-2p (Fig. 4D). On the other hand, we observed higher OTB-SO_3 signal when competed with DIR (Fig. 4E), indicative of partial OTB-SO_3 sensitivity to photobleaching (as previously measured). Thus, multi-selective scFvs may allow

fluorescence signal exchange when presented with a second fluorogen; however, the extent of color-switch depends upon the binding affinities of each fluorogen.

Measuring Multi-Color Surface Receptor Traffic on Live Cells

The potential of multi-color activation from a single reporter allows for advanced strategies of cellular detection. In this regard we transfected live mammalian cells with HL1.0.1-TO1 fused to ADRB2. Upon agonist molecule receptor stimulation we measured the receptor traffic from the cell surface towards cytoplasm using sequential pulse-chase in three colors. Here the overall all goal to measure cell surface receptor traffic in real-time via successful removal of surface staining, but maintenance of staining in the internalized receptors. Thus, we first labelled the cells with DIR – the weakest affinity binding fluorogen – and followed by presenting a small molecule receptor agonist, isoproterenol. Post-internalization traffic, the cells were washed and relabeled with OTB-SO_3 fluorogen. The same process was repeated again and followed by labelling with TO1-2p. In this case, we were able to determine spatial and temporal locations of ADRB2 receptors using live cells in real-time (Fig. 5). Furthermore, we also noted that fluorogen removal via a wash-step and then followed by exchange resulted in faster relabeling of the cell surface receptors, rather than direct competition (compare to Fig. 4). As a result we performed single reporter tri-color fluorescence imaging to track in real time the spatial and temporal location of cell surface receptors.

Discussion

The properties of high affinity and specificity from single-chain-variable-fragments (scFvs) for a target ligands generates highly stable and functional scFv-fluorogen biosensors. As demonstrated in this report, in certain cases a single scFv molecule may target multiple different fluorogens from the same chemical family. Our fluorescence screen showed a high percentage activation, greater than 50 percent of diverse fluorogens analogs, against scFv HL1.0.1-TO1 (see Fig. 1). Accordingly, we propose that antibody multi-selectivity may prove more common in settings of small molecule targets rather than conventional antibody antigens, such as peptides or proteins. For the latter case, macromolecules possess a larger affinity interface that must be occluded from the

surrounding solvent, and results in lower energetically favorable conditions for binding. Here, the proteins and peptides possess geometric conformations and structural features that restrict the number of possible spatial orientations for binding when compared to small molecules. Also, macromolecules are subject to long range affinity interactions (i.e. electrostatic, hydrogen bonds, and hydrophobic) that may indirectly influence protein affinity and the specificity interface (Janin, 1997; Schreiber and Fersht, 1995). While conversely, long range interactions also negatively influence whole protein affinity associations via charge repulsions and/or unfavorable dipole orientations (Lockless and Ranganathan, 1999; Tompa, 2002). On the other hand, fluorogen molecules possess small and flexible scaffolds that offer a greater range of protein surface interactions – increased freedom of contact regions and geometrical orientations. Furthermore, small molecules tend to bury within the affinity binding region, which fully encapsulates the fluorogen from bulk-solvent and increases the free-energy conditions (i.e. lower entropy) for affinity binding (Bogan and Thorn, 1998).

Our findings further show that when comparing fluorogen analogs for scFv activation altered molecular electrostatics reveal a propensity for affinity disruptions. That is, we detected diminished or absence of fluorescence signal when charged groups were substituted or whole molecule electrostatic distributions were modified (see figure 1A and 1B). In this regard, our findings suggest that electrical forces largely influence the free energy landscape for affinity binding of fluorogens, and minor disturbances at electrostatic interfaces lead in severe loss/poor binding. This observation is reflective of protein-protein interaction models, where the principles of charge-charge and charge-dipole interactions prove critical for thermodynamic stability and association kinetics (Dill, 1990; Janin, 1997; Schreiber and Fersht, 1996). On the other hand, fluorogen structural modifications, based on cyclic or methine group modifications, proved less detrimental in fluorescence signal loss. For example, when comparing TO1-2p versus OTB-SO_3 (smaller heterocycle group), or TO1-2p versus DIR (longer methine linker), in both cases we still observed scFv fluorogen activation, yet with reduced binding affinities (see Table 1). Taken together, our data hints that for antibody small

molecule interactions, the scFv binding region allows greater malleability of fluorogens with structural rather than electrostatic fluorogens modifications.

Furthermore, our experimental findings also correspond with meta-data studies based on affinity hot-spot regions that stabilize protein-protein interactions (Morrow and Zhang, 2012). More specifically, hot-spots show involvement in affinity steering of target molecules for docking, and show preferential enrichment of residues tyrosine, tryptophan, and arginine (Bogan and Thorn, 1998; Lise et al., 2011). As a result, here we propose that polar and charged interactions (such as arginine and others) must govern the free energy landscape of the fluorogen affinity interface with the scFv – thereby guiding and orienting the small molecule. Whereas aromatic residues in the protein binding region, such as tyrosine, tryptophan and others, may help stabilize the fluorogens via π-stacking, hydrogen bonding, and hydrophobic interactions. This assertion also corresponds with multiple other protein-protein affinity models that describe an early affinity complex that is further stabilized by a later precise docking stage (Chakrabarti and Janin, 2002; Schreiber and Fersht, 1995; Schreiber and Fersht, 1996).

In this report we presented a screening method for identifying multi-selective FAPs; and also we highlighted novel approaches of microscopy detection based on multi-color fluorescence. More specifically, when compared to conventional methods, a bipartite non-covalent platform offers increased flexibility for target molecule detection – in regards to temporal and spatial fluorescence. That is, contrary to ever present signal, such as fluorescent antibodies or reporter proteins, fluorescence detection remains absent until the addition of a cognate fluorogen to the cellular medium. Conversely, here we observed that fluorogen removal from the cellular medium results in fluorescence loss, and is regulated by affinity off-rates (Fig. 3). Application-wise, a tunable signal detection reporter offers opportunity for advanced protein discovery strategies involving protein turnover at the cellular membrane, pulse-chase of vesicular traffic, or post cell labeling assays that require the removal of signal (Bodor et al., 2012; Fuchs et al., 2010; Giepmans et al., 2006; Lippincott-Schwartz and Patterson, 2003; Mizukami et al., 2012). Furthermore, in order to further accelerate the off-rates of signal detection using multi-selective FAPs, future focus will be placed on

isolating weak affinity fluorogens. Here, two distinct engineering strategies may rapidly facilitate this: The site-directed mutagenesis of the protein scaffold, or chemical alterations of fluorogen sub-groups (Rastede et al., 2015; Shank et al., 2009; Yates et al., 2013; Zanotti et al., 2011).

A multi-color and selective scFv FAP offers increased user freedom when compared to covalent-based bipartite reporters, or standard fluorescent proteins. That is because a non-covalent affinity platform allows fluorescence signal manipulations via the kinetic tuning of fluorogen molecules in the surrounding medium. That is, a user may initially present a fluorogen to the cellular medium, and subsequently compete for binding via addition of a different color fluorogen. As demonstrated in this report, such fluorescence color manipulation is contingent upon the fluorogen affinities for the scFv. Here, the higher affinity fluorogens compete with weaker affinity fluorogens to force a new equilibrium, resulting in rapid exchange of fluorescence signals (see Fig 4). Incidentally, one may further accelerate color signal exchange via first removal of the first fluorogen from the medium (wash-off) followed by subsequent presentation of a second color fluorogen (as demonstrated in figure 5). Accordingly, a user may perform measurements of real-time signal exchange using different color channels – with direct application for cellular trafficking studies such as the downregulation and re-sensitization of cell surface receptors (Fisher et al., 2014; Wu et al., 2012; Wu et al., 2014). On the other hand, fluorogen competition, using similar affinity fluorogens, results in multi-color co-labelling instead of color-switch. Here, co-labelling may prove critical for the detection of targets with high background/noise – by method of signal overlap measurements using two independent channels.

In summary, the data presented in this report advances the field of fluorescence reporters, and reveals novel strategies of detection previously problematic or impossible using conventional methods. Furthermore, the work presented here offers proof-of-concept examples with direct implications for live cell detection strategies. Thus, here we seek to challenge the conventional paradigm and offer new directions in the field of fluorescent reporters.

Acknowledgements

We would like to thank H. Teng for confocal microscopy assistance. Also, B. Schmidt, N. Shank, E. Rastede, G. Silva, and other MBIC chemists for the synthesis of most of the fluorogens used in this report. We are grateful to A. Dempsey and C. Szent-Gyorgyi for providing the HL1-TO1 and HL1.0.1-TO1 surface displayed yeast cell lines and yeast cell culture reagents. The National Institutes of Health National supported this work, grant U54GM103529.

Abbreviations: single-chain-variable-fragment (scFv), fluorogen-activating proteins (FAPs), adrenoreceptor-beta-2 (ADRB2), phosphate-buffer-saline (PBS), Oxazole-Thiazole-Blue derivative (OTB-SO_3), Thiazole-Orange derivative (TO1-2p), Dimethyl-Indole-Red (DIR), Foster-resonance energy transfer (FRET).

The authors have declared no conflict of interest.

References

Bodor, D. L., Rodríguez, M. G., Moreno, N., Jansen, L. E. T., Bodor, D. L., Rodríguez, M. G., Moreno, N. and Jansen, L. E. T. (2012). Analysis of Protein Turnover by Quantitative SNAP-Based Pulse-Chase Imaging. In *Current Protocols in Cell Biology*, p. 8.8.1-8.8.34. Hoboken, NJ, USA: John Wiley & Sons, Inc.

Bogan, A. A. and Thorn, K. S. (1998). Anatomy of hot spots in protein interfaces. *J. Mol. Biol.* **280**, 1–9.

Brun, M. A., Tan, K.-T., Nakata, E., Hinner, M. J. and Johnsson, K. (2009). Semisynthetic Fluorescent Sensor Proteins Based on Self-Labeling Protein Tags. *J. Am. Chem. Soc.* **131**, 5873–5884.

Brun, M. A., Griss, R., Reymond, L., Tan, K.-T., Piguet, J., Peters, R. J. R. W., Vogel, H. and Johnsson, K. (2011). Semisynthesis of Fluorescent Metabolite Sensors on Cell Surfaces. *J. Am. Chem. Soc.* **133**, 16235–16242.

Cabantous, S., Pédelacq, J. D., Mark, B. L., Naranjo, C., Terwilliger, T. C. and Waldo, G. S. (2005a). Recent advances in GFP folding reporter and split-GFP solubility reporter technologies. Application to improving the folding and solubility of recalcitrant proteins from Mycobacterium tuberculosis. *J. Struct. Funct. Genomics* **6**, 113–119.

Cabantous, S., Terwilliger, T. C. and Waldo, G. S. (2005b). Protein tagging and detection with engineered self-assembling fragments of green fluorescent protein. *Nat. Biotechnol.* **23**, 102–107.

Chakrabarti, P. and Janin, J. (2002). Dissecting protein-protein recognition sites. *Proteins Struct. Funct. Genet.* **47**, 334–343.

Chen, I., Howarth, M., Lin, W. and Ting, A. Y. (2005). Site-specific labeling of cell surface proteins with biophysical probes using biotin ligase. *Nat. Methods* **2**, 99–104.

Constantin, T. P., Silva, G. L., Robertson, K. L., Hamilton, T. P., Waggoner, A. S., Armitage, B. A. and Fague, K. (2008). Synthesis of new fluorogenic cyanine dyes and incorporation into RNA fluoromodules. *Org. Lett.* **10**, 1561–4.

Dill, K. A. (1990). Dominant forces in protein folding. *Biochemistry* **29**, 7133–7155.

Fernández-Suárez, M., Baruah, H., Martínez-Hernández, L., Xie, K. T., Baskin, J. M., Bertozzi, C. R. and Ting, A. Y. (2007). Redirecting lipoic acid ligase for cell surface protein labeling with small-molecule probes. *Nat. Biotechnol.* **25**, 1483–1487.

Fisher, G. W., Adler, S. A., Fuhrman, M. H., Waggoner, A. S., Bruchez, M. P. and Jarvik, J. W. (2010). Detection and quantification of β2AR internalization in living cells using FAP-based biosensor technology. *J. Biomol. Screen.* **15**, 703–709.

Fisher, G. W., Fuhrman, M. H., Adler, S. A., Szent-Gyorgyi, C., Waggoner, A. S. and Jarvik, J. W. (2014). Self-Checking Cell-Based Assays for GPCR Desensitization and Resensitization. *J. Biomol. Screen.* **19**, 1220–1226.

Fuchs, J., Böhme, S., Oswald, F., Hedde, P. N., Krause, M., Wiedenmann, J. and Nienhaus, G. U. (2010). A photoactivatable marker protein for pulse-chase imaging with superresolution. *Nat. Methods* **7**, 627–630.

Gallo, E., Snyder, A. C. and Jarvik, J. W. (2015). Engineering tandem single-chain Fv as cell surface reporters with enhanced properties of fluorescence detection. *Protein Eng. Des. Sel.* **28**, 327–337.

Gautier, A., Juillerat, A., Heinis, C., Corrêa, I. R., Kindermann, M., Beaufils, F. and Johnsson, K. (2008). An Engineered Protein Tag for Multiprotein Labeling in Living Cells. *Chem. Biol.* **15**, 128–136.

Giepmans, B. N. G., Adams, S. R., Ellisman, M. H. and Tsien, R. Y. (2006). The Fluorescent Toolbox for Assessing Protein Location and Function. *Science (80-.).* **312**, 217–224.

Griffin, B. A., Adams, S. R. and Tsien, R. Y. (1998). Specific Covalent Labeling of\nRecombinant Protein Molecules\nInside Live Cells. *Science (80-.).* **281**, 269.

Holleran, J., Brown, D., Fuhrman, M. H., Adler, S. A., Fisher, G. W. and Jarvik, J. W. (2010). Fluorogen-activating proteins as biosensors of cell-surface proteins in living cells. *Cytom. Part A* **77**, 776–782.

Hori, Y., Ueno, H., Mizukami, S. and Kikuchi, K. (2009). Photoactive Yellow Protein-Based Protein Labeling System with Turn-On Fluorescence Intensity. *J. Am. Chem. Soc.* **131**, 16610–16611.

Irwin Chen, Yoon-Aa Choi, and and Ting*, A. Y. (2007). Phage Display Evolution of a Peptide Substrate for Yeast Biotin Ligase and Application to Two-Color Quantum Dot Labeling of Cell Surface Proteins.

Janin, J. J. (1997). The Kinetics of Protein-Protein Recognition. *Proteins Struct. Funct. Genet.* **28**, 153–161.

Kent, K. P., Oltrogge, L. M. and Boxer, S. G. (2009). Synthetic Control of Green Fluorescent Protein. *J. Am. Chem. Soc.* **131**, 15988–15989.

Keppler, A., Gendreizig, S., Gronemeyer, T., Pick, H., Vogel, H. and Johnsson, K. (2002). A general method for the covalent labeling of fusion proteins with small molecules in vivo. *Nat. Biotechnol.* **21**, 86–89.

Keppler, A., Pick, H., Arrivoli, C., Vogel, H. and Johnsson, K. (2004). Labeling of fusion proteins with synthetic fluorophores in live cells. *Proc. Natl. Acad. Sci. U. S. A.* **101**, 9955–9.

Kosaka, N., Ogawa, M., Choyke, P. L., Karassina, N., Corona, C., McDougall, M., Lynch, D. T., Hoyt, C. C., Levenson, R. M., Los, G. V., et al. (2009). *In Vivo* Stable Tumor-Specific Painting in Various Colors Using Dehalogenase-Based Protein-Tag Fluorescent Ligands. *Bioconjug. Chem.* **20**, 1367–1374.

Laura Vivero-Pol, §, Nathalie George, †, Holger Krumm, †, Kai Johnsson, *,† and and Nils Johnsson*, § (2005). Multicolor Imaging of Cell Surface Proteins.

Lee, H. D., Lord, S. J., Iwanaga, S., Zhan, K., Xie, H., Williams, J. C., Wang, H., Bowman, G. R., Goley, E. D., Shapiro, L., et al. (2010). Superresolution Imaging of Targeted Proteins in Fixed and Living Cells Using Photoactivatable Organic Fluorophores. *J. Am. Chem. Soc.* **132**, 15099–15101.

Lippincott-Schwartz, J. and Patterson, G. H. (2003). Development and Use of Fluorescent Protein Markers in Living Cells. *Science (80-.).* **300**, 87–91.

Lise, S., Buchan, D., Pontil, M. and Jones, D. T. (2011). Predictions of hot spot residues at protein-protein interfaces using support vector machines. *PLoS One* **6**,.

Liu, D. S., Nivón, L. G., Richter, F., Goldman, P. J., Deerinck, T. J., Yao, J. Z., Richardson, D., Phipps, W. S., Ye, A. Z., Ellisman, M. H., et al. (2014). Computational design of a red fluorophore ligase for site-specific protein labeling in living cells. *Proc. Natl. Acad. Sci. U. S. A.* **111**, E4551-9.

Lockless, S. W. and Ranganathan, R. (1999). Evolutionarily Conserved Pathways of Energetic Connectivity in Protein Families. *Science (80-.).* **286**,.

Los, G. V., Encell, L. P., McDougall, M. G., Hartzell, D. D., Karassina, N., Zimprich, C., Wood, M. G., Learish, R., Ohana, R. F., Urh, M., et al. (2008). HaloTag: A novel protein labeling technology for cell imaging and protein analysis. *ACS Chem. Biol.* **3**, 373–382.

Luedtke, N. W., Dexter, R. J., Fried, D. B. and Schepartz, A. (2007). Surveying polypeptide and protein domain conformation and association with FlAsH and ReAsH. *Nat. Chem. Biol.* **3**, 779–784.

Masuda, H., Takenaka, Y., Yamaguchi, A., Nishikawa, S. and Mizuno, H. (2006). A novel yellowish-green fluorescent protein from the marine copepod, Chiridius poppei, and its use as a reporter protein in HeLa cells. *Gene* **372**, 18–25.

Matz, M. V., Fradkov, A. F., Labas, Y. A., Savitsky, A. P., Zaraisky, A. G., Markelov, M. L. and Lukyanov, S. A. (1999). Fluorescent proteins from nonbioluminescent Anthozoa species. *Nat. Biotechnol.* **17**, 969–973.

Mizukami, S., Watanabe, S., Akimoto, Y. and Kikuchi, K. (2012). No-Wash Protein Labeling with Designed Fluorogenic Probes and Application to Real-Time Pulse-Chase Analysis. *J. Am. Chem. Soc.* **134**, 1623–1629.

Morrow, J. K. and Zhang, S. (2012). Computational prediction of protein hot spot residues. *Curr. Pharm. Des.* **18**, 1255–65.

Özhalici-Ünal, H., Pow, C. L., Marks, S. A., Jesper, L. D., Silva, G. L., Shank, N. I., Jones, E. W., Burnette, J. M., Berget, P. B. and Armitage, B. A. (2008). A rainbow of fluoromodules: A promiscuous scFv protein binds to and activates a diverse set of fluorogenic cyanine dyes. *J. Am. Chem. Soc.* **130**, 12620–12621.

Pham, H. H., Szent-Gyorgyi, C., Brotherton, W. L., Schmidt, B. F., Zanotti, K. J., Waggoner, A. S. and Armitage, B. A. (2015). Bichromophoric dyes for wavelength shifting of dye-protein fluoromodules. *Org. Biomol. Chem.* **13**, 3699–3710.

Prasher, D. C., Eckenrode, V. K., Ward, W. W., Prendergast, F. G. and Cormier, M. J. (1992). *Primary structure of the Aequorea victoria green-fluorescent protein*.

Rajapakse, H. E., Gahlaut, N., Mohandessi, S., Yu, D., Turner, J. R. and Miller, L. W. (2010). Time-resolved luminescence resonance energy transfer imaging of protein-protein interactions in living cells. *Proc. Natl. Acad. Sci. U. S. A.* **107**, 13582–7.

Rastede, E. E., Tanha, M., Yaron, D., Watkins, S. C., Waggoner, A. S. and Armitage, B. a (2015). Spectral fine tuning of cyanine dyes: electron donor-acceptor substituted analogues of thiazole orange. *Photochem. Photobiol. Sci.* **14**, 1703–12.

Robers, M., Pinson, P., Leong, L., Batchelor, R. H., Gee, K. R. and Machleidt, T. (2009). Fluorescent labeling of proteins in living cells using the FKBP12 (F36V) tag. *Cytom. Part A* **75A**, 207–224.

Sample, V. and Newman, R. (2009). The structure and function of fluorescent proteins. *Chem. Soc. Rev.* **38**, 2852–64.

Saunders, M. J., Szent-Gyorgyi, C., Fisher, G. W., Jarvik, J. W., Bruchez, M. P. and Waggoner, A. S. (2012). Fluorogen activating proteins in flow cytometry for the study of surface molecules and receptors. *Methods* **57**, 308–317.

Saunders, M. J., Liu, W., Szent-Gyorgyi, C., Wen, Y., Drennen, Z., Waggoner, A. S. and Meng, W. S. (2013). Engineering fluorogen activating proteins into self-assembling materials. *Bioconjug. Chem.* **24**, 803–810.

Saunders, M. J., Block, E., Sorkin, A., Waggoner, A. S. and Bruchez, M. P. (2014). A bifunctional converter: Fluorescein quenching scFv/Fluorogen activating protein for photostability and improved signal to noise in fluorescence experiments. *Bioconjug. Chem.* **25**, 1556–1564.

Saurabh, S., Zhang, M., Mann, V. R., Costello, A. M. and Bruchez, M. P. (2015). Kinetically Tunable Photostability of Fluorogen-Activating Peptide-Fluorogen Complexes. *ChemPhysChem* **16**, 2974–2980.

Schreiber, G. and Fersht, a R. (1995). Energetics of protein-protein interactions: analysis of the barnase-barstar interface by single mutations and double mutant cycles. *J. Mol. Biol.* **248**, 478–486.

Schreiber, G. and Fersht, A. R. (1996). Rapid, electrostatically assisted association of proteins. *Nat. Struct. Biol.* **3**, 427–31.

Shagin, D. A., Barsova, E. V, Yanushevich, Y. G., Fradkov, A. F., Lukyanov, K. A., Labas, Y. A., Semenova, T. N., Ugalde, J. A., Meyers, A., Nunez, J. M., et al. (2004). GFP-like Proteins as Ubiquitous Metazoan Superfamily: Evolution of Functional Features and Structural Complexity. *Mol. Biol. Evol.* **21**, 841–850.

Shaner, N. C., Campbell, R. E., Steinbach, P. A., Giepmans, B. N. G., Palmer, A. E. and Tsien, R. Y. (2004). Improved monomeric red, orange and yellow fluorescent proteins derived from Discosoma sp. red fluorescent protein. *Nat. Biotechnol.* **22**, 1567–72.

Shaner, N. C., Steinbach, P. A. and Tsien, R. Y. (2005). A guide to choosing fluorescent proteins. *Nat. Methods* **2**, 905–909.

Shank, N. I., Zanotti, K. J., Lanni, F., Berget, P. B. and Armitage, B. A. (2009). Enhanced photostability of genetically encodable fluoromodules based on fluorogenic cyanine dyes and a promiscuous protein partner. *J. Am. Chem. Soc.* **131**, 12960–12969.

Shank, N. I., Pham, H. H., Waggoner, A. S. and Armitage, B. A. (2013). Twisted cyanines: A non-planar fluorogenic dye with superior photostability and its use in a protein-based fluoromodule. *J. Am. Chem. Soc.* **135**, 242–251.

Shimomura, O., Johnson, F. H. and Saiga, Y. (1962). Extraction, purification and properties of aequorin, a bioluminescent protein from the luminous hydromedusan, Aequorea. *J. Cell. Comp. Physiol.* **59**, 223–39.

Silva, G. L., Ediz, V., Yaron, D. and Armitage, B. A. (2007). Experimental and computational investigation of unsymmetrical cyanine dyes: Understanding torsionally responsive fluorogenic dyes. *J. Am. Chem. Soc.* **129**, 5710–5718.

Szent-Gyorgyi, C., Schmidt, B. A. F., Schmidt, B. A. F., Creeger, Y., Fisher, G. W., Zakel, K. L., Adler, S., Fitzpatrick, J. A. J., Woolford, C. A., Yan, Q., et al. (2008). Fluorogen-activating single-chain antibodies for imaging cell surface proteins. *Nat. Biotechnol.* **26**, 235–40.

Szent-Gyorgyi, C., Schmidt, B. F., Fitzpatrick, J. A. J. and Bruchez, M. P. (2010). Fluorogenic dendrons with multiple donor chromophores as bright genetically targeted and activated probes. *J. Am. Chem. Soc.* **132**, 11103–11109.

Szent-Gyorgyi, C., Stanfield, R. L., Andreko, S., Dempsey, A., Ahmed, M., Capek, S., Waggoner, A. S., Wilson, I. A. and Bruchez, M. P. (2013). Malachite green mediates homodimerization of antibody VL domains to form a fluorescent ternary complex with singular symmetric interfaces. *J. Mol. Biol.* **425**, 4595–4613.

Tompa, P. (2002). Intrinsically unstructured proteins. *Trends Biochem. Sci.* **27**, 527–533.

Uttamapinant, C., White, K. A., Baruah, H., Thompson, S., Fernández-Suárez, M., Puthenveetil, S. and Ting, A. Y. (2010). A fluorophore ligase for site-specific protein labeling inside living cells. *Proc. Natl. Acad. Sci. U. S. A.* **107**, 10914–9.

Vasilev, K. V, Gallo, E., Shank, N. and Jarvik, J. W. (2016). Novel biosensor of membrane protein proximity based on fluorogen activated proteins. *Comb. Chem. High Throughput Screen.* **19**, 392–399.

Wombacher, R., Heidbreder, M., van de Linde, S., Sheetz, M. P., Heilemann, M., Cornish, V. W. and Sauer, M. (2010). Live-cell super-resolution imaging with trimethoprim conjugates. *Nat. Methods* **7**, 717–719.

Wu, Tapia, Fisher, Simons, Strouse, Foutz, Waggoner, Jarvik and Sklar (2012). Discovery of regulators of receptor internalization with high-throughput flow cytometry. *Mol. Pharmacol.* **82**, 645–657.

Wu, Y., Tapia, P. H., Jarvik, J., Waggoner, A. S., Sklar, L. A., Wu, Y., Tapia, P. H., Jarvik, J., Waggoner, A. S. and Sklar, L. A. (2014). Real-Time Detection of Protein Trafficking with High-Throughput Flow Cytometry (HTFC) and Fluorogen-Activating Protein (FAP) Base Biosensor. In *Current Protocols in Cytometry*, p. 9.43.1-9.43.11. Hoboken, NJ, USA: John Wiley & Sons, Inc.

Yao, J. Z., Uttamapinant, C., Poloukhtine, A., Baskin, J. M., Codelli, J. A., Sletten, E. M., Bertozzi, C. R., Popik, V. V. and Ting, A. Y. (2012). Fluorophore Targeting to Cellular Proteins via Enzyme-Mediated Azide Ligation and Strain-Promoted Cycloaddition. *J. Am. Chem. Soc.* **134**, 3720–3728.

Yates, B. P., Peck, M. A. and Berget, P. B. (2013). Directed evolution of a fluorogen-activating single chain antibody for function and enhanced brightness in the cytoplasm. *Mol. Biotechnol.* **54**, 829–841.

Yushchenko, D. A., Zhang, M., Yan, Q., Waggoner, A. S. and Bruchez, M. P. (2012). Genetically Targetable and Color-Switching Fluorescent Probe. *ChemBioChem* **13**, 1564–1568.

Zanotti, K. J., Silva, G. L., Creeger, Y., Robertson, K. L., Waggoner, A. S., Berget, P. B. and Armitage, B. a (2011). Blue fluorescent dye-protein complexes based on fluorogenic cyanine dyes and single chain antibody fragments. *Org. Biomol. Chem.* **9**, 1012–20.

Zürn, A., Klenk, C., Zabel, U., Reiner, S., Lohse, M. J. and Hoffmann, C. (2010). Site-Specific, Orthogonal Labeling of Proteins in Intact Cells with Two Small Biarsenical Fluorophores. *Bioconjug. Chem.* **21**, 853–859.

Figures

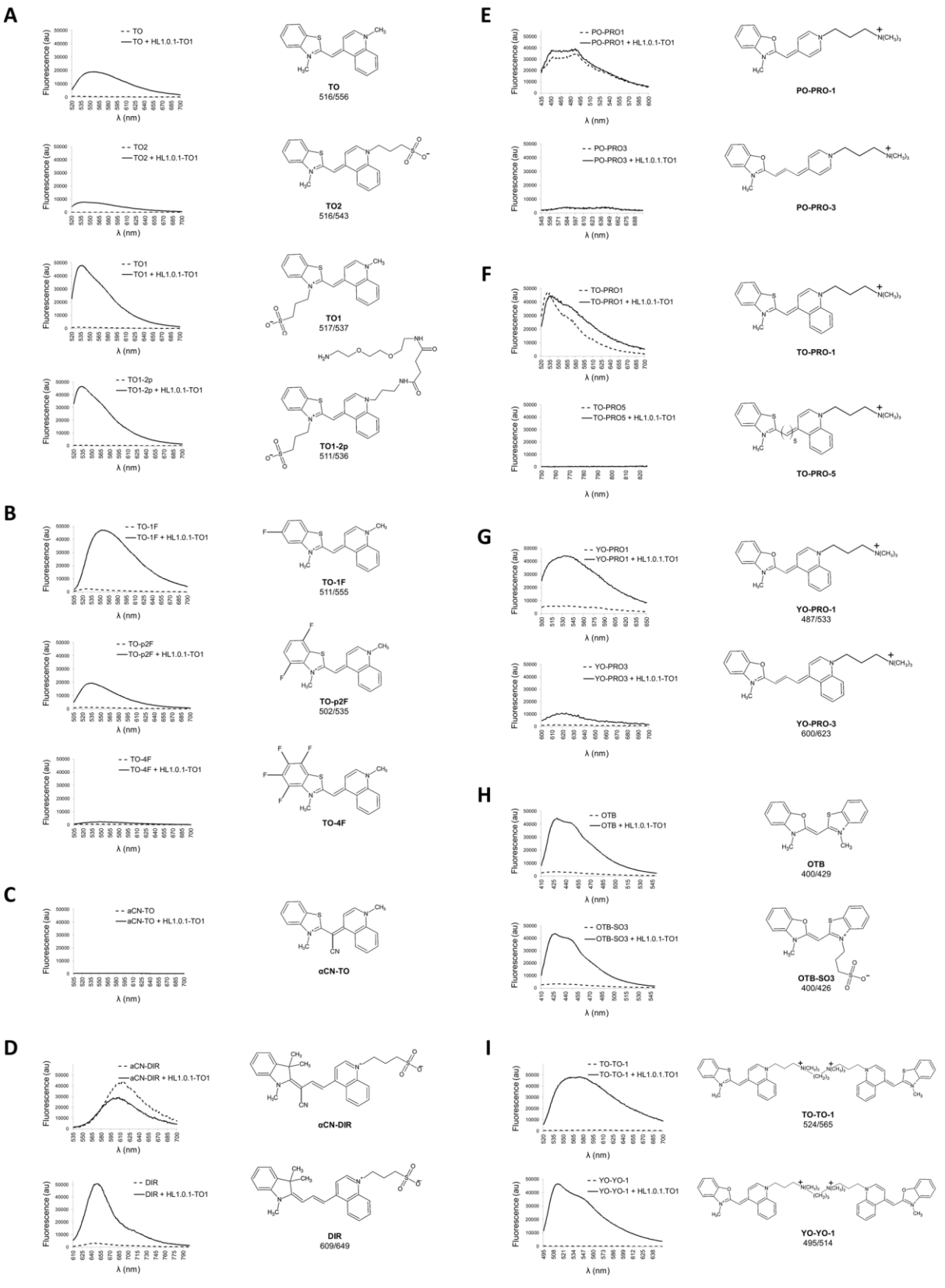

Figure 1. A fluorescence activation screen using HL1.0.1-TO1 protein against diverse cyanine family fluorogens. All measurements were performed in PBS using triplicate samples with 500 nM fluorogen and HL1.0.1-TO purified protein. We included the excitation and emission maxima for the fluorogens that exhibit fluorescence activation listed below the name of its corresponding fluorogen.

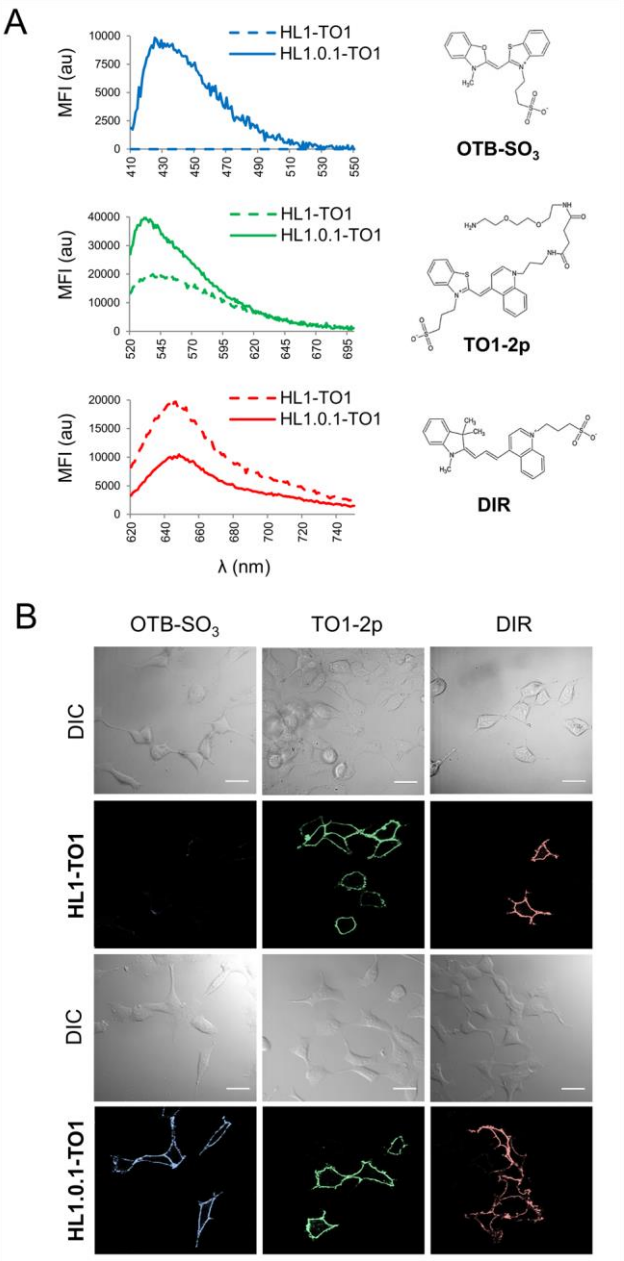

Figure 2. Comparison of HL1-TO1 or HL1.0.1-TO1 proteins expressed at the surface of live cells and screened for activation of different fluorogens. (A) Fluorescence emission spectra of surface displayed HL1-TO1 versus HL1.0.1-TO1 on yeast cells in presence of different fluorogens. Comparisons assessments were performed at 2- or 5-fold the KD values of each fluorogen for its cognate scFv (see Table 1). (B) Micrographs of live mammalian cells expressing HL1.0.1-TO1 fused to adrenoreceptor beta-1 (ADRB2) at the surface. Cells were imaged in the presence of 100 nM of each fluorogen independently with the micrographs scale bar set at 30 μm.

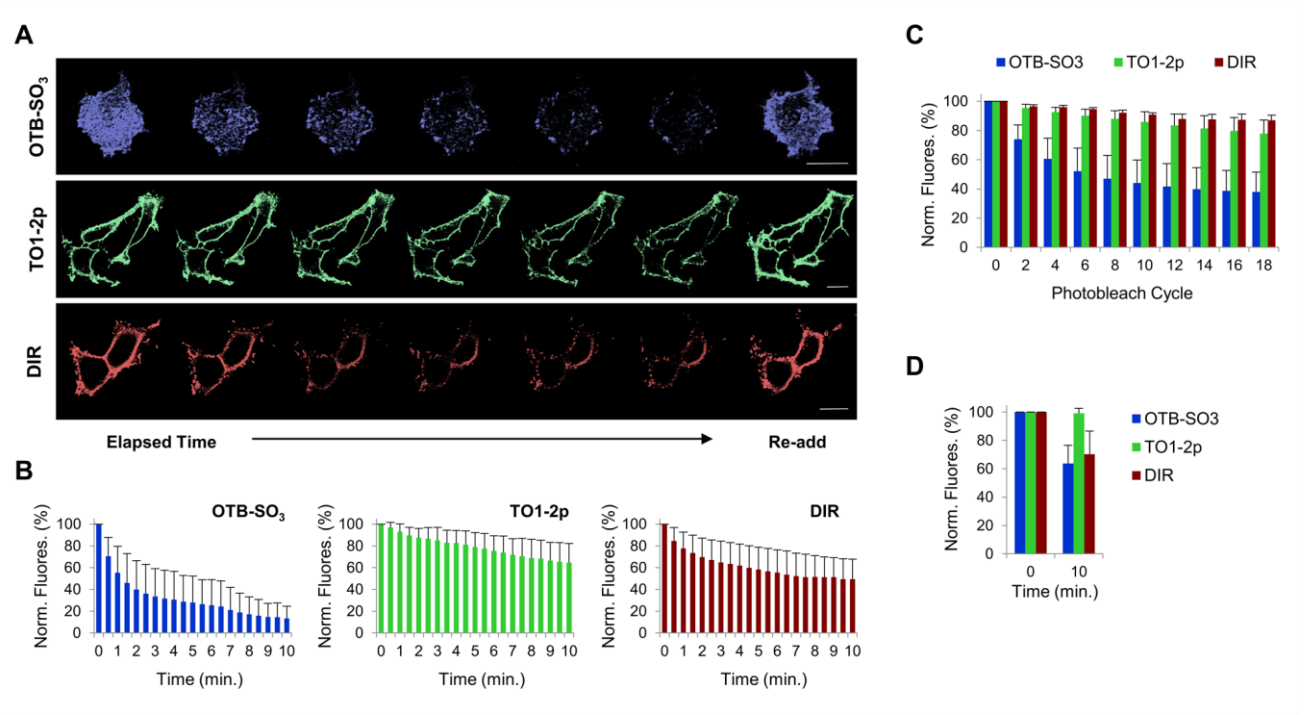

Figure 3. Assessing fluorescence signal loss at the surface of live mammalian cells post fluorogen removal from the cellular medium. All analyses were performed using cells expressing HL1.0.1-TO1 fused to ADRB2 at the cell surface. (A) Time-lapse micrographs from cells initially labelled with fluorogen, then washed and imaged for 10 minutes; at the last time point fluorogen was re-added. (B) Bar graph summary of fluorescence intensities from fluorogen removal time-lapse images (n=5). (C) Bar graph summary of fluorescence intensities from photobleached time-lapse images in presence of fluorogen (n=5). (D) Bar graph summary of fluorescence intensities from images at only two time points after fluorogen removal (n=5). All assays were performed with 100 nM of each fluorogen, and the error bars denote standard deviation from the mean. Each fluorogen time-series micrograph represents multiples images over time, with the scale bar set at 15 μm.

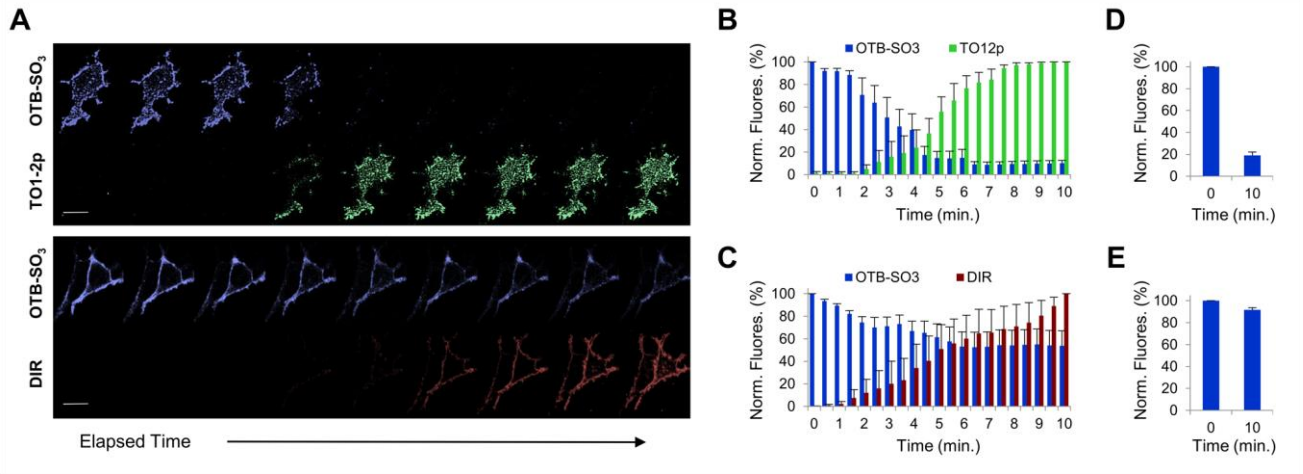

Figure 4. Determining fluorescence signal exchange at the surface of live cell via two fluorogen competition. All analyses were performed using mammalian cells expressing HL1.0.1-TO1 fused to ADRB2 at the cell surface. (A) Time-lapse micrographs from cells initially labelled with OTB-SO_3 fluorogen, then presented in the medium with either TO1-2p or DIR fluorogens and immediately time-lapse imaged for 10 minutes. Note, we observed improved image resolutions at longer wavelength emissions due to reduced cellular background and higher laser excitation power settings. (B) Bar graph summary of fluorescence intensities from fluorogen competition time-lapse images of OTB-SO_3 vs. TO1-2p. The TO1-2p signal was normalized to the last time point fluorescence values. (C) Bar graph summary of fluorescence intensities from fluorogen competition time-lapse images of OTB-SO_3 vs. DIR. The DIR signal was normalized to the last time point fluorescence values. (D) Bar graph summary of OTB-SO_3 fluorescence at only two time points after addition of TO1-2p in the medium. (E) Bar graph summary of OTB-SO_3 fluorescence at only two time points after addition of DIR in the medium. All assays were performed in presence of 100 nM of each fluorogen, and each bar graph analysis was determined from n=5 images for each group, with error bars denoting standard error from the mean. Each fluorogen time-series micrograph represents multiples images over time, with the scale bar set at 15 μm.

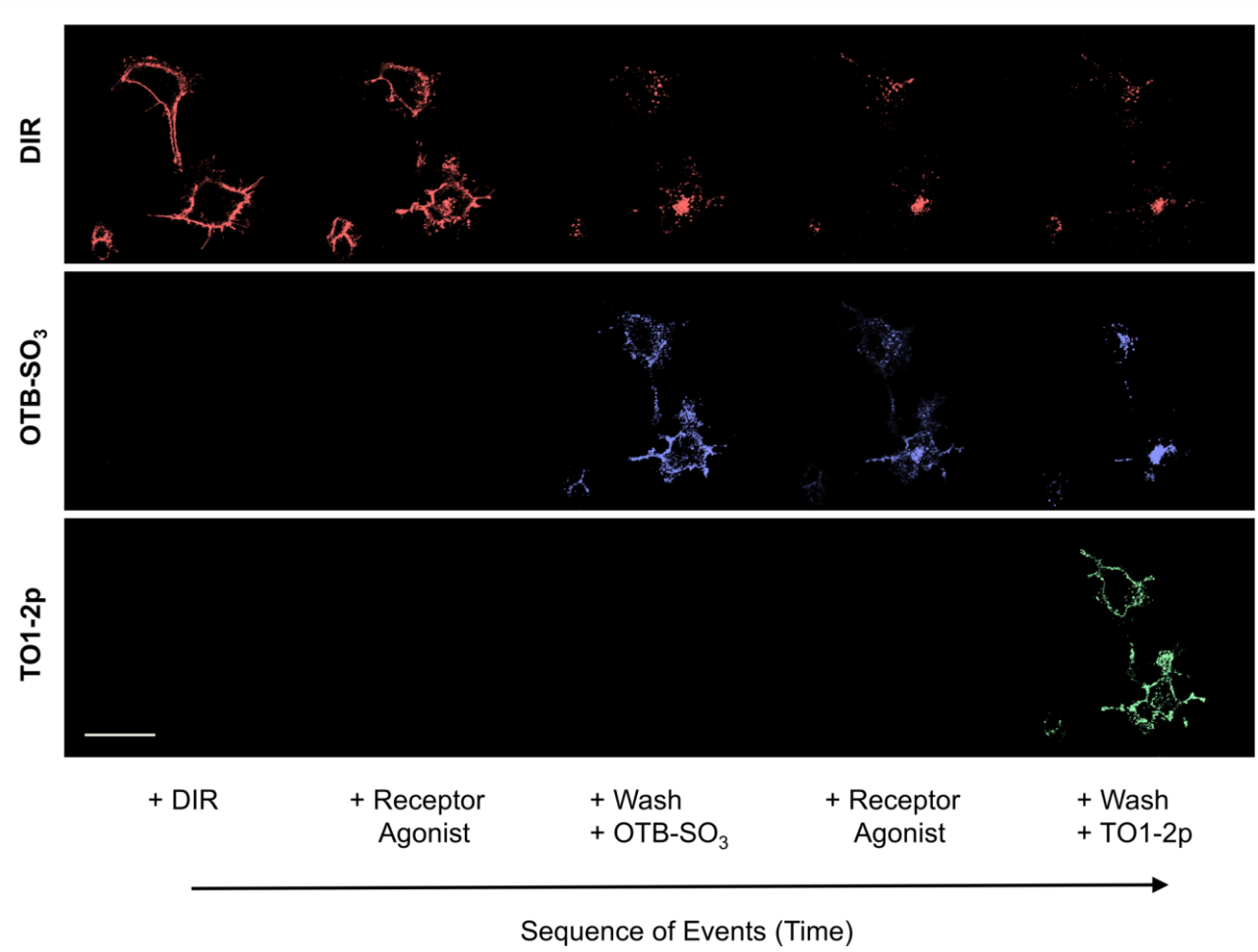

Figure 5. Imaging the real-time intracellular traffic response of cell surface receptors via three-color fluorogen sequential labeling. Mammalian cells expressing HL1.0.1-TO1 fused to ADRB2 at the surface were initially labelled using 100 nM DIR in the medium and subsequently presented with an ADRB2 agonist ligand (isoproterenol). The cells were washed with PBS and labeled with 50 nM OTB-SO_3 and the ADRB2 agonist. Subsequently, the cells were washed with PBS and then labeled with 500 nM TO1-2p. Each fluorogen time-series micrograph represents multiples images over time, with the scale bar set at 30 μm.

Table 1. Fluorogen excitation/emission maxima and Kd affinities for HL1-TO1 and HL1.0.1-TO1.

Fluorogen	HL1-TO1 Ex/Em (λmax/nm)	HL1.0.1-TO1 Ex/Em (λmax/nm)	HL1-TO1 K_D (nM)	HL1.0.1-TO1 K_D (nM)
OTB-SO_3	-	400/426	-	51.8
TO1-2p	510/527 [a]	511/536	360 [a]	2.6
DIR	607/649	609/649	442 [b]	565

a. Szent-Gyorgyi et al., 2008
b. Ozhalici-Unal et al., 2008

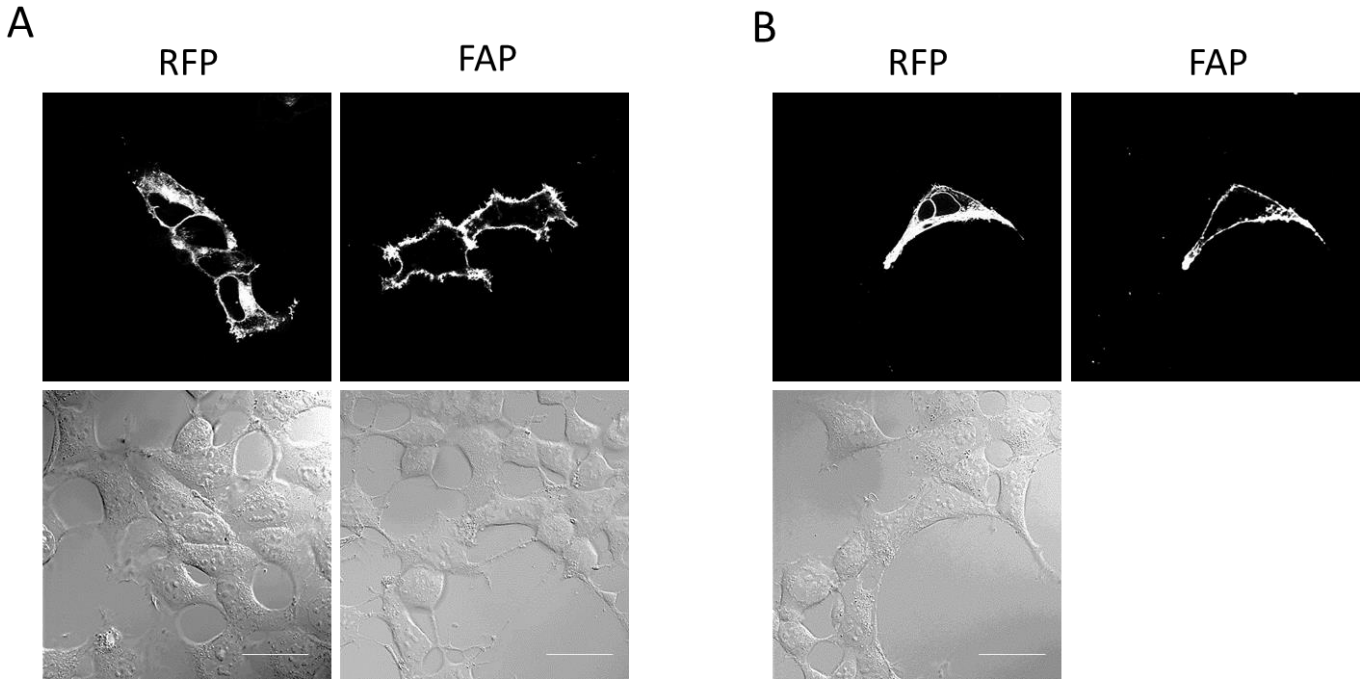

Supplemental Figure 1. Micrograph comparisons of cell surface displayed fluorescent protein RFP versus scFv FAP. (A) Images of cells transfected with either RFP or HL1.0.1-TO1 FAP genetically fused to the N'-terminus of the PDGFR transmembrane domain region. FAP labelled cells were measured in the presence of TO1-2p fluorogen in the medium. (B) Images of cells transfected with an N-terminus HL1.0.1-TO1 FAP-tagged to RFP and genetically fused to the PDGFR transmembrane domain region. The cells were measured in the presence of TO1-2p fluorogen in the medium. The scale bar represent 30 um.

>HL1-TO1

QVQLVESEAEVKKPGSSVKVSCKASGGTFSSYAISWVRQAPGQGLEWMGGIIPIFGTANYAQKF
QGRVTITADESTSTAYMELSSLRSEDTAVYYCVLLDTTMVTGYYFDYWGQGTLVTVSSGILGSG
GGGSGGGGSGGGGSNFMLTQPPSASGTPGQSVTISCSGSGSNIGNNKVNWYQQLPGTAPKLLIY
SNNQRPSGVPDRFSGSKSGTSASLAISGLQSEDEADYYCAAWDDSLNGYVFGTGTKLTVL

>HL1.0.1-TO1

QVQLVESEAEVKKPGSSVKVSCKASGGTFSSYAISWVRQAPGQGLEWMGG**T**IPIFGTA**D**YAQ**E**F
QGRVTIT**T**DESTSTAYMELS**G**LRSEDTAVYYCVLL**G**TTMVTG**H**YFDYWGQGTLVTVSSGILGSG
GGGSGGGGSGGGGSNFMLTQPPSASGTPGQSVTISCSGSGSNIGNNKVNWYQQLPGTAPKLLIY
SNNQRPSGVPDRFSGSKSGTSASLAISGLQSEDEADYYCAAWDD**G**L**S**GYVFGTGTKLTVL

Supplemental Figure 2. Amino acid sequences of scFv FAPs used in this report with red highlighted letters indicating mutations in the affinity matured versus parent scFv.

Fluorogen	Excitation (nm)	Emission (nm)	Signal / Background
OTB	400	429	13.69
OTB-SO3	400	426	12.79
PO-Pro1	438	459	1.23
BO-Pro1	458	480	2.87
YO-Pro1	487	533	7.67
YO-YO-1	495	514	182.30
TO-4F	495	551	4.11
TO-p2F	502	535	17.45
TO-1F	511	555	30.72
TO1-2p	511	536	173.84
aCN-TO	513	N/A	N/A
TO	516	556	45.68
TO2	516	543	67.06
TO1	517	537	121.17
TO-TO-1	524	565	78.89
aCN-DIR	525	N/A	N/A
PO-Pro3	539	N/A	N/A
YO-Pro3	600	623	8.18
DIR	609	649	18.35
TO-Pro5	745	N/A	N/A

Supplemental Figure 3. Fluorescence excitation/emission maxima using purified protein HL1.0.1-TO1 and different fluorogen analogs.

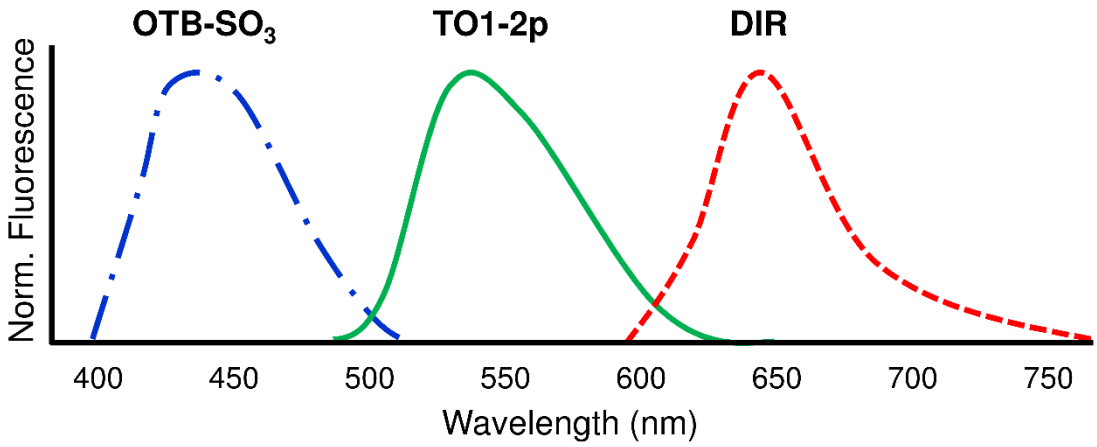

Supplemental Figure 4. Comparing fluorescence emission spectra of each fluorogen with scFv HL1.0.1-TO1.

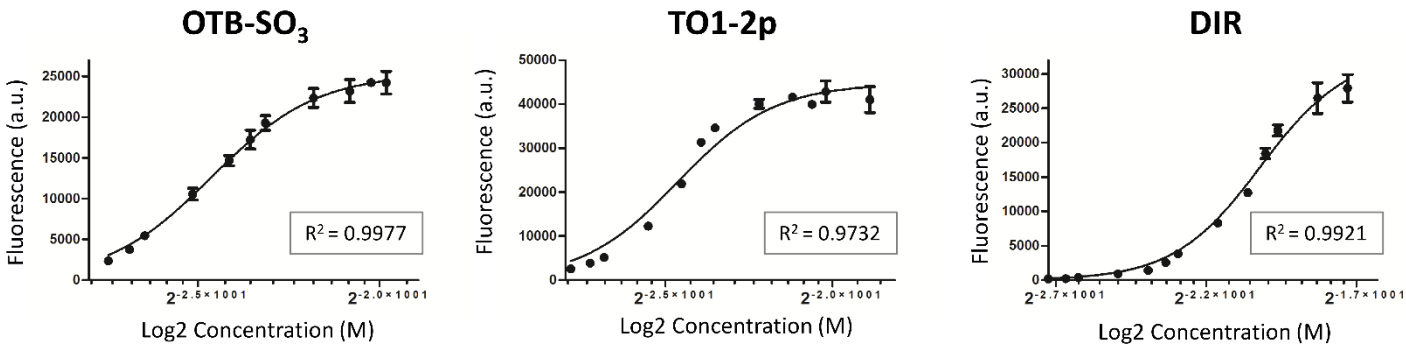

Supplemental Figure 5. Titration graphs of each fluorogen with surface displayed HL1.0.1-TO1 yeast cells.